Incommensurate Spin Fluctuations in High–Transition Temperature Superconductors

B. O. Wells, Y. S. Lee, M. A. Kastner, R. J. Christianson, R. J. Birgeneau,* K. Yamada, Y. Endoh, G. Shirane

Neutron scattering experiments have revealed a fascinating interplay between the hole doping, the spin fluctuations, and the superconductivity of the cuprate superconductors. Recently, electrochemical techniques have been used to produce large single crystals of La_2CuO_{4+y}, which has mobile oxygen dopants. Staging behavior of the excess oxygen has been demonstrated, and the low-energy spin fluctuations in stage 6 La_2CuO_{4+y} have been measured. The spin fluctuations are incommensurate with the lattice and have spatial, energy, and temperature dependencies very much like those in $La_{2-x}Sr_xCuO_4$, with similar high transition temperature. This establishes the universality of the incommensurate spin fluctuations among the La_2CuO_4-based superconductors.

After a decade of intensive research, it has become clear that the phenomenon of high transition temperature (high-T_c) superconductivity exhibits both great complexity and rich physics. It appears that all high-T_c superconductors are based on structures with square-planar copper oxide layers. One of the most striking features of the copper oxide superconductors is that they are all derived from charge-doping antiferromagnetic insulators. These undoped parent compounds have one hole per copper site, thereby yielding one unpaired spin on each copper ion. The copper spins align at low temperatures into three-dimensional antiferromagnetic long-range order. Upon doping to ~1.05 to 1.25 holes per copper site, the lamellar copper oxide materials become superconducting with short-range magnetic order.

The insulating parent compounds are interesting in themselves. Standard one-electron band theory predicts that they should be nonmagnetic metals, which is clearly incorrect. Thus the parent compounds are Mott-Hubbard insulators, materials that standard theories say should be metallic but in fact are insulating due to correlations among localized electrons. A great deal of progress has been made in understanding these insulators: The magnetism is well described by conventional theory, and proper models have been identified for the electronic structure. However, the physics of the doped superconductors is much more complex, and little consensus has been reached as to the correct physical description of this system. Clearly, a better experimental guide to the physics of these materials must be achieved. Some necessary features of such a guide include (i) the use of the simplest possible materials that show the desired physical properties, (ii) the determination of which physical properties are universally present in high-T_c materials, and (iii) identification of the relations between atomic structure, magnetism, and electronic properties in a given material by performing complete sets of experiments on the same compounds.

As part of our efforts to fulfill the experimental goals listed above, we have pursued an extensive experimental analysis project on the La_2CuO_{4+y} system (*1*). As we have shown previously and summarize below, this material has an elaborate series of structural phases that are fascinating in their own right. Here we report inelastic magnetic neutron scattering studies of superconducting $La_2CuO_{4.055}$. Of particular importance is the comparison of the magnetic excitations in the La_2CuO_{4+y} compound with those in $La_{2-x}Sr_xCuO_4$ (*2*). Both materials are based on the original parent compound La_2CuO_4, but the nature of the dopant ions and the structures are fundamentally different. The Sr^{2+} dopants in $La_{2-x}Sr_xCuO_4$ enter the structure substitutionally for La^{3+} ions, whereas the oxygen dopants in La_2CuO_{4+y} occupy interstitial sites (*3*, *4*). Hence, the Sr^{2+} ions are essentially immobile once the crystal solidifies below ~1400 K, whereas the excess oxygen dopants in La_2CuO_{4+y} remain mobile down to near 200 K (*1*, *3*, *4*), which is much smaller than the important magnetic and electronic energies which are the antiferromagnetic exchange coupling between nearest neighbor Cu spins $J \simeq 1500$ K and the electronic bandwidth $W \simeq 2J$. Therefore, over the experimentally investigated temperature range ($T < 400$ K) the disorder caused by the randomly substituted Sr^{2+} ions is "quenched" in that the immobile ions cannot reorder into an equilibrium arrangement. However, the mobile O^{2-} ions will participate in the system's thermodynamics, arranging themselves so as to minimize the free energy to the extent that their mobility permits. Thus any disorder caused by the intercalated oxygen is "annealed" with respect to the major energetics of the system. Therefore, a comparison of the two systems allows us to test the effect of quenched versus annealed disorder on the properties of a given high-T_c system.

As we shall demonstrate, the magnetic excitations in the two systems turn out to be remarkably similar in their magnitudes and their spatial, energy, and temperature dependencies in the normal and superconducting states. This surprising robustness of the spin fluctuations suggests that they are an essential property of the idealized doped CuO_2 layer and therefore must be basic features of all candidate theories of high-T_c superconductivity.

Phase diagram and structures. The phase diagram for $La_{2-x}Sr_xCuO_4$ (*5*) and that which we have determined for La_2CuO_{4+y} are shown in Fig. 1. A comparison of the two reveals some obvious similarities: The undoped parent compound is an antiferromagnetic insulator, initial doping lowers the antiferromagnetic ordering temperature T_N, and at higher doping levels both become superconductors. However, there are clear, fundamental differences between the two. The phase diagram for La_2CuO_{4+y} has many miscibility gaps and a wider variety of structures than that for $La_{2-x}Sr_xCuO_4$. The reason for this, as noted above, is the mobility of the O^{2-} intercalant ions. Thus, the O^{2-} ions phase-separate into oxygen-rich and oxygen-poor regions; further, concentrations between integer stagings appear to phase-separate as well. The phase separation between $y \simeq 0.01$ and $y \simeq 0.055$ (Fig. 1B) has been extensively explored before our work (*3*, *4*).

As a result of a concerted materials effort, we have learned how to grow and electrochemically intercalate large, narrow mosaic single crystals of La_2CuO_{4+y} with y up to ~ 0.1 and volumes approaching 0.5 cm^3. This has enabled us to elucidate the basic structures of the materials using neutron scattering. Neutrons have no charge but possess a magnetic moment. Thus they only interact weakly with matter: scattering off of atomic nuclei via the strong force or

B. O. Wells, Y. S. Lee, M. A. Kastner, R. J. Christianson, R. J. Birgeneau, Department of Physics, Massachusetts Institute of Technology (MIT), Cambridge, MA 02139, USA.
K. Yamada and Y. Endoh, Department of Physics, Tohoku University, Aramaki Aoba, Sendai, 980-77, Japan.
G. Shirane, Department of Physics, Brookhaven National Laboratory, Upton, NY 11973, USA.
*To whom correspondence should be addressed.

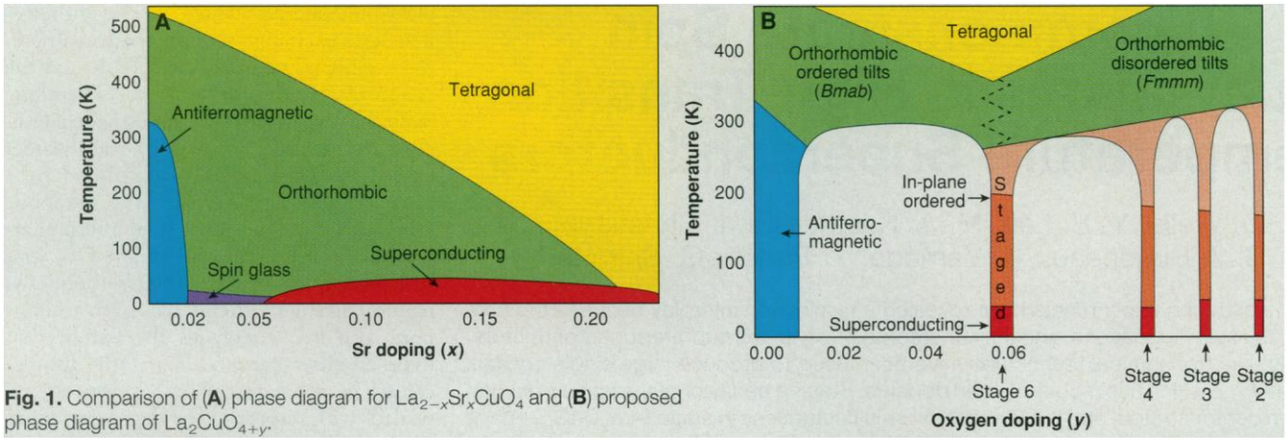

Fig. 1. Comparison of (**A**) phase diagram for $La_{2-x}Sr_xCuO_4$ and (**B**) proposed phase diagram of La_2CuO_{4+y}.

magnetic moments via a dipole-dipole interaction. Therefore, neutrons require relatively large samples for appreciable scattering, but for the same reason they are not surface sensitive—which makes them ideal for probing bulk collective behavior of crystals. In a neutron scattering experiment, neutrons may diffract from a static ordering of nuclei or spins. For such a process, the neutrons do not transfer energy to the sample; hence this process is called elastic scattering. The other possibility is for neutrons to diffract from a temporally fluctuating ordering of nuclei or spins, resulting in energy transferred to or from the sample, which is termed inelastic scattering. Due to the small cross section for inelastic magnetic scattering, large single crystals are essential to investigate the spin fluctuations in samples of superconducting La_2CuO_{4+y}. The experimental details are the same as those we reported previously (*1*). For simplicity in discussing the magnetic neutron scattering we shall use the high-temperature tetragonal *I4/mmm* unit cell rather than the low-temperature orthorhombic *Bmab* unit cell of the undoped La_2CuO_4 compound. The tetragonal **c** axis is perpendicular to the CuO_2 planes, and the **a** and **b** axes are within the plane as shown in the unit cell diagram in Fig. 2A. In reciprocal space, the (*H*,*K*,*L*) components for the **q** positions are given in units of ($2\pi/a$, $2\pi/b$, $2\pi/c$).

We begin by discussing the previously reported oxygen phase separation region from $y = 0.01$ to 0.055 in the phase diagram for La_2CuO_{4+y}. Detailed neutron diffraction studies (*1*) of samples with $0.01 < y < 0.055$ show that below $T_{PS} \simeq 290$ K the samples phase-separate into an oxygen-poor phase with $y \simeq 0.01$ and an oxygen-rich phase with $y \simeq 0.055$. The former is an antiferromagnetic insulator with $T_N \simeq 250$ K, whereas the latter is a superconductor with $T_c \simeq 32$ K. From the diffraction peaks, we infer that the regions that make up each phase are large in all directions, greater than about 1000 Å.

The oxygen-poor phase of La_2CuO_{4+y} ($y \leq 0.01$) has the same low-temperature orthorhombic structure as undoped La_2CuO_4 described by the *Bmab* space group. The schematic in Fig. 2B indicates the tilting of the CuO_6 octahedra present in this structure; it is this tilting that determines the *Bmab* symmetry. However, for the oxygen-rich phase ($y \geq 0.055$), we find that the low-temperature orthorhombic structure has an additional superlattice modulation along the **c** axis (*1*). The diffraction is consistent with a structural model originally proposed for $La_2NiO_{4+\delta}$ (6). We present a schematic for this proposed structure in Fig. 2C. Within the planes, the tilts of the CuO_6 octahedra are ordered in the same manner as those in undoped La_2CuO_4, and perpendicular to the planes the tilts have the same local ordering. The structure of La_2CuO_{4+y} with $y \geq 0.055$ differs from that of La_2CuO_4 in that the oxygen-rich material contains broad antiphase domain boundaries parallel to the CuO_2 planes and regularly spaced along the **c** axis. The antiphase domain boundaries consist of layers across which the direction of the CuO_6 tilts is reversed. The antiphase domain boundaries are presumed to be caused by ordered layers of interstitial oxygen. Flipping a single octahedron will cause the reversed state to propagate throughout the plane because the octahedra share corner oxygen atoms. This will have the effect of creating an entire plane of favorable interstitial sites for the intercalated oxygen. Such a one-dimensional ordering of the extra oxygen is similar to the staging behav-

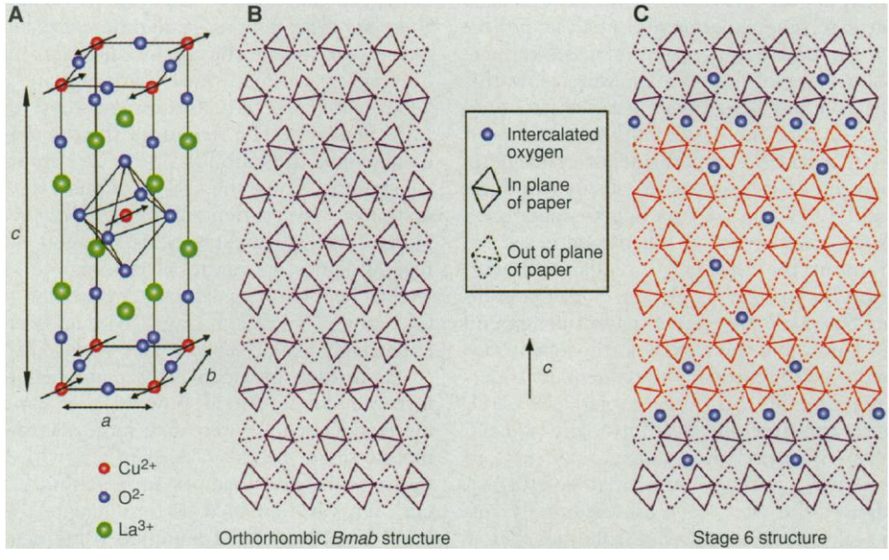

Fig. 2. Structural diagrams. (**A**) The tetragonal unit cell of La_2CuO_{4+y}. The arrows on the copper atoms represent their spins. (**B**) Schematic for the CuO_6 octahedra tilt structure of undoped La_2CuO_4. (**C**) Schematic for the CuO_6 octahedra tilt structure of stage 6 La_2CuO_{4+y}. The different shades for the octahedra correspond to different antiphase tilt domains.

ior of halogens and alkalis intercalated into graphite. Following the literature on intercalated graphite, we use the term "staging" to describe the **c**-axis modulation of the undoped structure; stage n refers to an induced periodicity of n CuO_2 host layers. Noninteger staging numbers for a sample may be derived from mixtures of integer-staged domains.

Two features of these staged structures should be noted. First, there is as yet no direct diffraction evidence that the excess oxygen itself is staged. The scattering peaks we measure come from the antiphase boundaries of the octahedra tilts. Such a configuration certainly creates planes of favorable interstitial sites, which favor the staging of oxygen, but we have not been able to measure scattering peaks directly from the interstitial oxygen. Second, the boundaries between the two oppositely tilted regions cannot be as sharp as those depicted in Fig. 2C. Such a configuration would lead to scattering from higher harmonics. In fact, typically only the first harmonic signal is detected above the background; accordingly, we conclude that the boundary must be smeared out with the arrangement of tilts more like a sine wave. A sinusoidal modulation of the intercalated oxygen layers along **c** would then be expected. The lack of direct scattering from planes of intercalated oxygen may be explained by such a more homogenous distribution of oxygen.

For excess oxygen concentrations between ~0.01 and ~0.055, the behavior as a function of temperature is quite elaborate. As mentioned above, phase separation occurs below $T_{PS} \simeq 290$ K. However, the onset of stage ordering in the oxygen-rich phase occurs at a lower temperature near 255 K. If the sample is cooled through the temperature region around 210 K over a period of several hours, as recently reported by Xiong *et al.* (*7*), an additional phase transition occurs. This transition corresponds to the establishment of a mass density modulation along a direction in the CuO_2 plane at 45° to the Cu-Cu nearest neighbor direction with a periodicity of about 61 Å (*1*). Increasing y beyond 0.055 results in samples with, in succession, stage $n = 4$, 3, and 2. The exact oxygen concentration y for each of these stages is not yet known, nor is the superconducting T_c, although preliminary evidence suggests that T_c for $n = 2$ may be as high as 45 K.

Clearly, the La_2CuO_{4+y} system represents a rich system for the study of structural, magnetic, transport, and superconducting properties.

Spin fluctuations. Considerable effort has gone into studying the spin fluctuations in the high-T_c superconductors and related compounds (*5*, *8*, *9*), in part because the magnetism is fundamental to many theoretical models of the superconductivity. Indeed, understanding the magnetism of the undoped parent compounds has been one of the significant successes in the field (*8*, *10*). While the superconductors themselves show no long-range ordered magnetism of the Cu moments, there are clear short-range antiferromagnetic correlations (*8*, *9*, *11*). The mechanism of the disruption of the long-range order by holes is still under debate.

The best and most extensive data exist for the $La_{2-x}Sr_xCuO_4$ system (*8*, *9*, *11*). Neutron scattering studies have shown that antiferromagnetic spin fluctuations exist over a broad range of x (*8*). As a function of doping the magnetic peak positions, intensities, and correlation lengths show an intriguing evolution starting from the well-understood insulating antiferromagnet, which exhibits three-dimensional Néel order for $0 \leq x \leq 0.0175$. At higher doping for $0.02 \leq x < 0.05$, the neutron scattering peaks indicate short-range magnetic order with the characteristic antiferromagnetic wavevector (1/2, 1/2) independent of the L direction normal to the CuO_2 planes (*12*). However, in the doping regime where superconductivity appears, for $x \gtrsim 0.05$, the spin fluctuations no longer occur at (1/2, 1/2) but split into four peaks located at (1/2 ± δ, 1/2) and (1/2, 1/2 ± δ) (Fig. 3A).

Neutron scattering experiments have also determined that for optimally doped $La_{2-x}Sr_xCuO_4$ (that is, with $x = 0.15$ and $T_c \simeq 38$ K) in the superconducting state, the intensities of the spin fluctuations below 3.5 meV at (1/2 ± δ, 1/2) and (1/2, 1/2 ± δ) are suppressed, vanishing as $T \rightarrow 0$ (*2*), indicating that a magnetic gap forms below the superconducting transition temperature. Earlier work on underdoped $La_{2-x}Sr_xCuO_4$ samples ($x < 0.15$) with $T_c \simeq 33$ K has shown that the low-energy neutron scattering peaks are also suppressed at the above **q** positions, but the intensity does not go to zero at the lowest temperatures studied (*8*, *9*, *13*). The energy range for which spin scattering is suppressed in these lower T_c samples is similar to that where a complete gap is seen in the optimally doped sample. Understanding this magnetic gap in the superconducting state depends on both a complete experimental determination of its behavior and an understanding of the origin of the magnetic peaks in the normal state.

There are many models that may account for the incommensurate splitting of the inelastic magnetic scattering peaks in $La_{2-x}Sr_xCuO_4$. Two of the most widely discussed are the nested Fermi surface model (*14*–*16*) and the charge fluctuation model. In the Emery and Kivelson version of the latter model (*17*), the doped holes segregate into one-dimensional local metallic stripes that act as antiphase domain boundaries between the remaining undoped, antiferromagnetic regions. There is extensive ongoing research to determine if either of these two physical pictures or other proposed models is correct. Empirically, it must be determined whether the effect seen in $La_{2-x}Sr_xCuO_4$ is universal among different compounds with different types of dopants and how the effect develops as a function of doping. The experiments that we discuss here add to the empirical knowledge base in both of these areas.

Figure 3A shows a schematic of the trajectory for the scans we use to measure the incommensurate magnetic peaks. The scattering rods are at (1/2 ± δ, 1/2, L) and (1/2, 1/2 ± δ, L) in the tetragonal notation. The

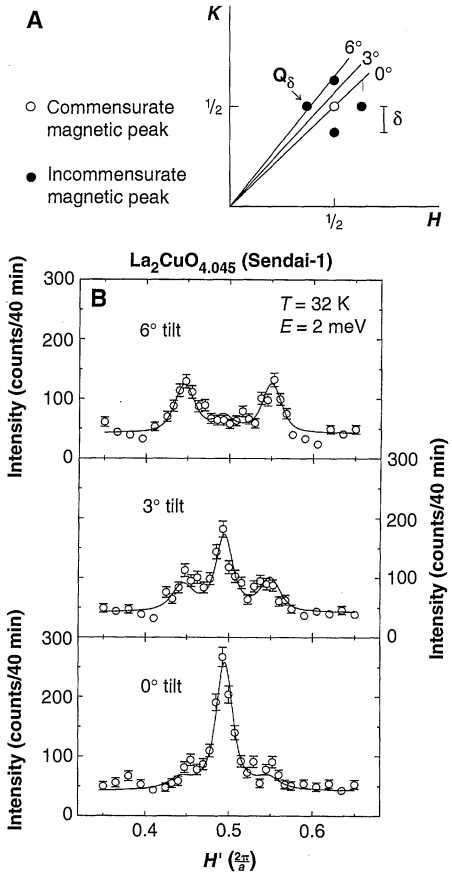

Fig. 3. (**A**) Position of the inelastic magnetic peaks in reciprocal space. The scan trajectories for three different tilt angles (θ_t) are shown. The path for each trajectory is given by $\{H'[\cos(\theta_t) - \sin(\theta_t)], H'[\cos(\theta_t) + \sin(\theta_t)], -0.6\}$. (**B**) Inelastic scans on Sendai-1. The tilt of the scan trajectory is varied from 0° to 3° to 6°, whereas the temperature and energy transfer are fixed at $T = 32$ K and $E = 2$ meV. The lines are fits to the cross section that includes the (1/2, 1/2) peak and the four incommensurate peaks, where only the tilt angle is changed between panels.

slight orthorhombicity at low temperatures, while relevant to the structural characteristics, is irrelevant to the magnetic properties. The alignment of the crystal is such that the (*H*,*H*,*L*) zone is in the scattering plane. Thus, to scan over the incommensurate peaks we must scan outside of the (*H*,*H*,*L*) zone. This is accomplished by tilting the sample by 6° as shown in Fig. 3A. Because we are studying two-dimensional scattering that gives rise to rods along the *L* direction, the value of *L* is immaterial except for purposes of maximizing the signal-to-background (*11*, *13*).

Our inelastic magnetic scattering experiments on La_2CuO_{4+y} have been performed on two single crystal samples. Both have been intercalated with oxygen by use of electrolysis at 90°C in a D_2O solvent in contrast to the H_2O solvent used in our previous studies (*1*). One sample (labeled Sendai-1 after the institution at which it was grown) has a mass of 3.366 g and an oxygen doping within the first miscibility gap region with ~80% of the sample on the oxygen-rich side at low temperatures; that is, it has the approximate composition $La_2CuO_{4.045}$, with a superconducting onset temperature of T_c = 32 K. The other sample (labeled MIT-1) weighs 1.927 g with an oxygen content just at the oxygen-rich edge of the first miscibility gap, having the approximate composition $La_2CuO_{4.055}$, with T_c = 31 K. These samples are less than one-third the size of the crystals used for the best inelastic neutron scattering measurements on $La_{2-x}Sr_xCuO_4$. However, they are about 10 times larger than most of the crystals used in previous electrochemical oxygen intercalation studies. Our inelastic neutron scattering experiments were carried out at the H7 triple-axis spectrometer at the Brookhaven High Flux Beam Reactor.

The oxygen-rich portion of Sendai-1 has a staging number of 6.0 at low temperatures, whereas the oxygen-rich portion of MIT-1 is predominantly stage 6.2 with a small admixture of stage 4.1. Figure 3B shows longitudinal scans in **q** at an energy transfer of 2 meV for the Sendai-1 sample at different tilt angles. A tilt angle of 0° is equivalent to scanning along *H* in the (*H*,*H*,*L*) zone, whereas increasing the tilt angle to around 6° corresponds to scanning through the position of two of the four incommensurate magnetic peaks. We see two different sets of peaks in these scans. There is a peak at (1/2, 1/2, *L*) seen most clearly in the 0° tilt scan, as well as peaks that are seen best in the 6° tilt scans at (1/2 −δ, 1/2, *L*) and (1/2, 1/2 + δ, *L*), where δ = 0.105. The peak at (1/2, 1/2, *L*) arises from spin waves in the oxygen-poor Néel-ordered portion of the crystal and those at (1/2 ± δ, 1/2, *L*) and (1/2, 1/2 ± δ, *L*) from spin fluctuations in the oxygen-rich portion.

Our goal is to study the oxygen-rich material; thus, the rest of the data we present come from MIT-1, the sample near the high-*y* edge of the first miscibility gap. In this sample we see very little inelastic scattering at the (1/2, 1/2, *L*) position, indicating that only a small fraction of the sample consists of undoped CuO_2 planes. In Fig. 4 we present the inelastic scattering peaks for an energy transfer of 2 meV at three representative temperatures T = 50, 32 ($\sim T_c$), and 11 K. The peak intensity appears to increase slightly as T is lowered from 50 to 32 K but then is substantially reduced at 11 K. Similar behavior is seen for data taken at an energy transfer of 3 meV, but any such diminution of intensity for an energy transfer of 4 meV is very slight. This corresponds closely to the results obtained by both the Brookhaven (*11*, *13*) and Risö (*9*) groups for $La_{2-x}Sr_xCuO_4$ samples with similar T_c.

In Fig. 5 we present a summary plot of the imaginary part of the susceptibility $\chi''(\mathbf{q} = \mathbf{Q}_\delta, \omega)$, which measures the strength of the magnetic excitations, versus temperature at three small energy transfers for both this sample of La_2CuO_{4+y} and the $La_{2-x}Sr_xCuO_4$ sample with similar suboptimal T_c used in (*11*) and (*13*). We obtain $\chi''(\mathbf{Q}_\delta, \omega)$ for $La_2CuO_{4.055}$ from the inelastic magnetic peak intensity at the incommensurate position (1/2 − δ, 1/2, *L*) by removing the thermal factor and then normalize our data to that for the $La_{2-x}Sr_xCuO_4$ sample (*11*) with a single multiplicative constant to give the best overall agreement. The results are nearly identical within the error bars for these two systems. It appears that the temperature dependence of the spin fluctuations does

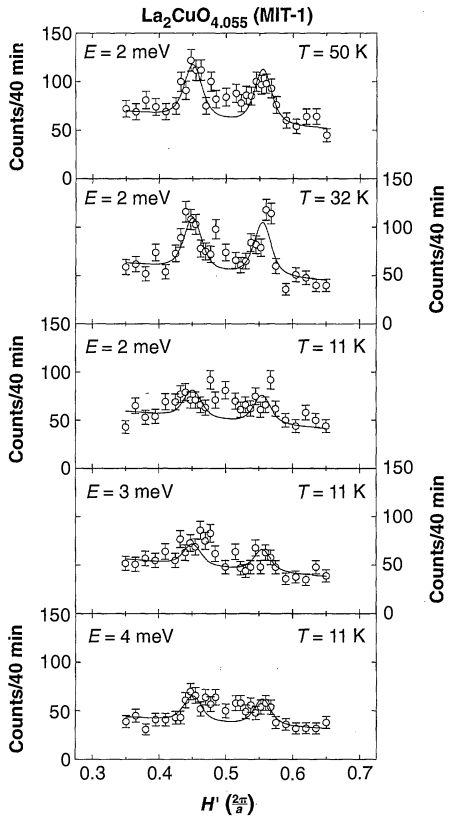

Fig. 4. Inelastic scans on MIT-1. The tilt of the scan trajectory is fixed at 6°, whereas the energy transfers and temperatures are varied. The lines are fits to the cross section that includes the four incommensurate peaks only.

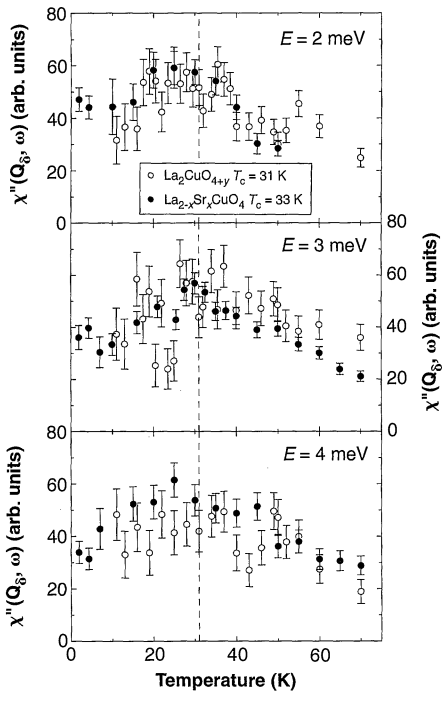

Fig. 5. The imaginary part of the susceptibility as a function of temperature for MIT-1 plotted with the data from (*11*) for a Sr^{2+}-doped crystal with similar T_c. A single multiplicative constant is used to normalize our data to give the best overall agreement. The dashed line corresponds to T_c = 31 *K*.

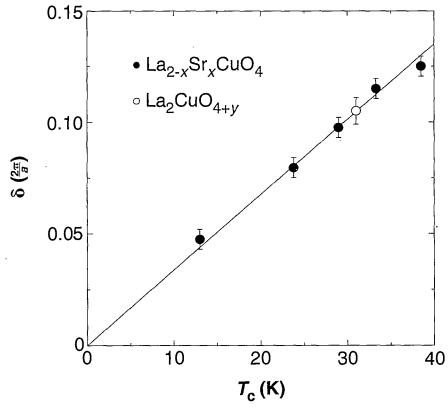

Fig. 6. The spin fluctuation incommensurability versus temperature data for $La_{2-x}Sr_xCuO_4$ obtained from Yamada *et al.* (*18*) with the datum point for our La_2CuO_{4+y} crystal MIT-1.

not depend on the nature of the dopants, Sr^{2+} versus O^{2-}, with their characteristic quenched versus annealed disorder. As the temperature is decreased toward the superconducting transition temperature, $\chi''(Q_\delta, \omega)$ increases, whereas below T_c the susceptibility levels off or decreases slightly. Although these two samples behave nearly identically, the temperature behavior of $\chi''(Q_\delta, \omega)$ depends on T_c for the $La_{2-x}Sr_xCuO_4$ system, where, as mentioned above, the optimally doped material with $T_c \simeq 38$ K exhibits a complete magnetic gap below 3.5 meV, whereas the underdoped materials with reduced T_c like those in Fig. 5 do not.

It is also instructive to compare the value of the incommensurability δ of the inelastic peaks for La_2CuO_{4+y} with that found for $La_{2-x}Sr_xCuO_4$. In recent work, Yamada *et al.*(*18*) have found a proportionality between the superconducting transition temperature and δ for highest quality single crystal samples up to optimal doping. Using the data from Yamada *et al.*, we have constructed a plot (Fig. 6) of δ versus T_c that includes our La_2CuO_{4+y} sample, which has $T_c = 31$ K and $\delta = 0.105$. It is clear from the figure that the La_2CuO_{4+y} sample fits perfectly on the straight line defined by the $La_{2-x}Sr_xCuO_4$ samples.

Conclusions. The most important conclusion of this work is that the existence of incommensurate spin fluctuations in the high-temperature superconductors is universal for materials based on La_2CuO_4. The most basic features of the spin fluctuations, their position in reciprocal space and evolution with temperature, appear to be independent of the type of dopant, the physical arrangement of the dopants, and the extent of disorder in the crystal. In the oxygen-doped La_2CuO_4 crystals, the excess oxygen can find its equilibrium arrangement down to temperatures near 200 K, which is well below the relevant magnetic and electronic energies in the system. This is quite different from the case for Sr^{2+} dopants, which are in fixed positions at the sample melting temperature near 1400 K.

These $La_2CuO_{4.055}$ data, as well as preliminary new data on high-quality single crystals of $La_{2-x}Sr_2CuO_4$ (*18*), suggest that the superconducting magnetic gap grows in both completeness and energy as the hole concentration is increased through the region of optimal doping. It is not clear how to reconcile this behavior of the magnetic gap with a simply evolving *d*-wave single-particle gap, or perhaps even more problematical, with suggestions of a pseudo-gap in underdoped samples as deduced from other probes. Finally, the suprising relation between T_c and the spin fluctuation incommensurability discovered by Yamada *et al.* (*18*) in $La_{2-x}Sr_xCuO_4$ and confirmed by us in $La_2CuO_{4.055}$ represents a challenge to all theories of high-T_c superconductivity. The physics of high-temperature superconductivity thus remains rich and complex but elusive.

REFERENCES AND NOTES

1. B. O. Wells *et al.*, *Z. Phys. B* **100**, 535 (1996); R. J. Birgeneau *et al.*, *Proceedings of the 10th Anniversary HTS Workshop on Physics, Materials, and Applications, Houston, TX* (World Scientific, Singapore, 1996).
2. K. Yamada *et al.*, *Phys. Rev. Lett.* **75**, 1626 (1995) and references therein.
3. J. D. Jorgensen *et al.*, *Phys. Rev. B* **38**, 11337 (1988).
4. D. C. Johnston *et al.*, *Phase Separation in Cuprate Superconductors*, E. Sigmund and K. A. Müller, Eds. (Springer-Verlag, Heidelberg, 1994), pp. 82–100.
5. R. J. Birgeneau and G. Shirane, *Physical Properties of High Temperature Superconductors*, D. M. Ginsberg, Ed. (World Scientific, Singapore, 1989), vol. 1, p. 152.
6. J. M. Tranquada *et al.*, *Phys. Rev. B* **50**, 6340 (1994).
7. X. Xiong *et al.*, *Phys. Rev. Lett.* **76**, 2997 (1996).
8. G. Shirane, R. J. Birgeneau, Y. Endoh, M. A. Kastner, *Physica B* **197**, 158 (1994); R. J. Birgeneau *et al.*, *J. Phys. Chem. Solids* **56**, 1913 (1995).
9. T. E. Mason, G. Aeppli, S. M. Hayden, A. P. Ramirez, H. A. Mook, *Phys. Rev. Lett.* **71**, 919 (1993).
10. M. Greven *et al.*, *Z. Phys. B* **96**, 465 (1995).
11. M. Matsuda *et al.*, *Phys. Rev. B* **49**, 6958 (1994). T_c is reduced in the sample used here both because of underdoping and possibly impurities; however, recent work has shown that the spin fluctuations measured in this sample are characteristic of the underdoped regime.
12. B. Keimer *et al.*, *Phys. Rev. B* **46**, 14034 (1992).
13. T. R. Thurston *et al.*, *ibid.*, p. 9128.
14. N. Bulut, D. Hone, D. J. Scalapino, N. E. Bickers, *Phys. Rev. Lett.* **64**, 2723 (1990).
15. Q. Si, Y. Zha, K. Levin, J. P. Lu, *Phys. Rev. B* **47**, 9055 (1993).
16. T. Tanamoto, H. Kohno, H. Fukuyama, *J. Phys. Soc.* **63**, 2739 (1994).
17. V. J. Emery and S. A. Kivelson, *Physica* **235–240**, 189 (1994).
18. K. Yamada *et al.*, unpublished data.

19. We thank F. C. Chou, M. Greven, and J. M. Tranquada for valuable discussions. The work at MIT was supported by the Materials Research Science and Engineering Center Program of the NSF under award number DMR 94-00334 and by the NSF under award number DMR 97-04532. Research at Brookhaven National Laboratory was carried out under contract No. DE-AC-2-76CH00016, Division of Material Science, U.S. Department of Energy. The work at Tohoku University was supported by a Grant-in-Aid for Scientific Research in Priority Areas and the U.S.–Japan Collaboration Program on Neutron Scattering sponsored by the Japanese Monbusho.

21 April 1997; accepted 3 July 1997